# Temperature dependence of magnetic anisotropy: An *ab initio* approach

J. B. Staunton,[1] L. Szunyogh,[2,3] A. Buruzs,[3] B. L. Gyorffy,[3,4] S. Ostanin,[1] and L. Udvardi[2,3]
[1]*Department of Physics, University of Warwick, Coventry CV4 7AL, United Kingdom*
[2]*Department of Theoretical Physics, Budapest University of Technology and Economics, Budapest, Hungary*
[3]*Centre for Computational Material Science, Technical University of Vienna, Getreidemarkt 9/134 A-1060, Vienna, Austria*
[4]*H.H.Wills Physics Laboratory, University of Bristol, Tyndall Avenue, Bristol BS8 1TL, United Kingdom*
(Received 8 June 2006; revised manuscript received 8 August 2006; published 17 October 2006)

We present a first-principles theory of the variation of magnetic anisotropy, $K$, with temperature, $T$, in metallic ferromagnets. It is based on relativistic electronic structure theory and calculation of magnetic torque. Thermally induced local moment magnetic fluctuations are described within the relativistic generalization of the disordered local moment theory from which the $T$ dependence of the magnetization, $m$, is found. We apply the theory to a uniaxial magnetic material with *tetragonal* crystal symmetry, $L1_0$-ordered FePd, and find its uniaxial $K$ consistent with a magnetic easy axis perpendicular to the Fe/Pd layers for all $m$ and proportional to $m^2$ for a broad range of values of $m$. This is the same trend that we have previously found in $L1_0$-ordered FePt and which agrees with experiment. We also study a magnetically soft *cubic* magnet, the $Fe_{50}Pt_{50}$ solid solution, and find that its small magnetic anisotropy constant $K_1$ rapidly diminishes from 8 $\mu$eV to zero. $K_1$ evolves from being proportional to $m^7$ at low $T$ to $m^4$ near the Curie temperature. The accounts of both the tetragonal and cubic itinerant electron magnets differ from those extracted from single ion anisotropy models and instead receive clear interpretations in terms of two ion anisotropic exchange.

DOI: 10.1103/PhysRevB.74.144411 PACS number(s): 75.30.Gw, 75.10.Lp, 71.15.Rf, 75.50.Bb

## I. INTRODUCTION

It is well-known that a description of magnetic anisotropy, $K$, can be provided once relativistic effects such as the spin-orbit coupling on the electronic structure of materials are considered. Over recent years first-principles theoretical work, based on relativistic density functional theory, has been quite successful in describing trends in $K$ for a range of magnetic materials in bulk, film and nanostructured form,[1–3] e.g., Refs. 4–9. These results can be fed into micromagnetic models of the magnetic properties to describe phenomena such as magnetization reversal processes in magnetic recording materials.[10] There are also implications for electronic transport effects such as anisotropic magnetoresistance (AMR).[11] Until only very recently, however, the temperature dependence of $K$ has not received a first-principles treatment and instead is generally assumed to follow that given by single ion anisotropy models developed by Callen and Callen and others over 40 years ago.[12] Here $K$ follows a simple power law dependence on the magnetization $m(T)$, so that $K(T) \propto m(T)^n$ where $n=3$ and $n=10$ for uniaxial and cubic magnets, respectively. The microscopic origin and nature of such power laws have recently been studied *ab initio* for the case study of the uniaxial magnet $L1_0$-FePt.[13,14] The unexpected dependence of the magnetic anisotropy of this magnet, found in experiment,[15–17] to decrease in proportion with the square of the magnetization, $m(T)$, is described well by the theoretical treatments whereas the single ion magnetic anisotropy models fail. Evidently the itinerant nature of the electrons in metallic magnets like FePt is an important factor.

In this paper we present a detailed description of our *ab initio* theory for the temperature dependence of magnetic anisotropy. This was applied for the first time to the $L1_0$-FePt case study and the results reported briefly.[13] The theory involves a fully relativistic description of the electronic structure and hence includes spin-orbit coupling effects. The thermally excited magnetic fluctuations are accounted for with the, by now, well-tried, disordered local moment (DLM) picture.[18–20] After describing the theory we discuss further applications to the uniaxial magnet $L1_0$-FePd and the cubic magnet disordered $Fe_{50}Pt_{50}$.

The study of temperature-dependent magnetic anisotropy has recently become particularly topical owing to extensive experimental studies of magnetic films and nanostructures and their technological potential. For example, fabrication of assemblies of increasingly smaller magnetic nanoparticles has great potential in the design of ultrahigh density magnetic data storage media.[21] If thermally driven demagnetization and loss of data is to be avoided over a reasonable storage period, there is, however, a particle size limit to confront. A way of reducing this limit is to use materials with high magnetocrystalline anisotropy, $K$, since the superparamagnetic diameter of a magnetic particle is proportional to $(k_BT/K)^{1/3}$, where $k_BT$ is the thermal energy.[22] Writing to media of very high $K$ material can be achieved by temporary heating.[16,23] $K$ is reduced significantly during the magnetic write process and the information is locked in as the material cools. Modelling this process and improving the design of high density magnetic recording media therefore requires an understanding of how $K$ varies with temperature.

The temperature dependence of magnetic anisotropy in magnets where the magnetic moments are well-localized, e.g., rare-earth and oxide magnets, is described rather well by these single ion anisotropy models but it is questionable whether this will also be the case for itinerant ferromagnets.[22] Owing to its high uniaxial magnetocrystalline anisotropy (MCA) ($4-10\times10^7$ ergs/cm$^3$ or up to 1.76 meV per FePt pair[24,25]) the chemically ordered $L1_0$ phase of equiatomic FePt, has attracted much attention as a potential ultrahigh magnetic recording density material.

 

Indeed arrays of FePt nanoparticles with diameters as small as 3 nm have been synthesized.[15,21] For a uniaxial magnet like this, $K$ is the difference between the free energies, $F^{(0,0,1)}$ and $F^{(1,0,0)}$ of the system magnetized along (0, 0, 1) and (1, 0, 0) crystallographic directions. So for the first application of our theory we chose $L1_0$-ordered FePt.[13] Careful experimental studies of its fundamental magnetic properties[15–17] find that over a large temperature range, $K(T)/K(0) = [m(T)/m(0)]^n$, where $n=2$ instead of $n=3$ as expected from the simple single ion anisotropy model. We found our *ab initio* calculations to be in good agreement with this surprising result. Mryasov *et al.*[14] independently examined the same issues with a different theoretical but complementary approach and drew the same conclusions. In this paper, after providing full details of the relativistic generalization of the disordered local moment (R-DLM) theory of magnetic anisotropy, we explore whether this $[m(T)/m(0)]^2$ behavior is a general property of the MCA of $L1_0$-ordered itinerant transition metal uniaxial magnets by investigating another important uniaxial magnetic material FePd. We also study the temperature dependence of a material which has cubic rather than the tetragonal crystal symmetry of $L1_0$-ordered alloys, and which is magnetically softer, namely compositionally disordered FePt.

In the next section we describe the temperature dependence of the magnetic anisotropy that emerges from classical spin models with single site anisotropy. We then review briefly current approaches to calculating $K$ from first-principles electronic theory of materials at $T=0$ K. An outline of the disordered local moment (DLM) picture of metallic magnetism at finite temperature precedes a description of its relativistic generalization. It is shown how the temperature dependence of the magnetization, $m(T)$, can be found. The key outcome from the R-DLM theory is the formalism for the magnetization dependence of magnetic anisotropy *ab initio*. Applications to uniaxial $L1_0$-FePd and cubic $Fe_{50}Pt_{50}$ follow and the final section provides a summary.

## II. SINGLE ION ANISOTROPY

The MCA of a material can be conveniently expressed as $K=\Sigma_\gamma K_\gamma g_\gamma(\hat{n})$ where the $K_\gamma$'s are coefficients, $\hat{n}$ is the magnetization direction and $g_\gamma$'s are polynomials (spherical harmonics) of the angles $\vartheta$, $\varphi$, fixing the orientation of $\hat{n}$ with respect to the crystal axes, and belong to the fully symmetric representation of the crystal point group. As the temperature rises, $K$ decreases rapidly. The key features of the results of the early theoretical work on this effect[12] are revealed by classical spin models pertinent to magnets with localized magnetic moments. The anisotropic behavior of a set of localized spins associated with ions sitting on crystalline sites, $i$, in the material, is given by a term in the Hamiltonian $H_{an}=\Sigma_i\Sigma_\gamma k_\gamma g_\gamma(\hat{e}_i)$ with $\hat{e}_i$ a unit vector denoting the spin direction on the site $i$. As the temperature is raised, the spins sample the energy surface over a small angular range about the magnetization direction and the anisotropy energy is given from the difference between averages taken for the magnetization along the easy and hard directions. If the coefficients $k_\gamma$ are assumed to be rather insensitive to temperature, the dominant thermal variation of $K$ for a ferromagnet is given by $K(T)/K(0)=\langle g_l(\hat{e})\rangle_T/\langle g_l(\hat{e})\rangle_0$. The averages $\langle\cdots\rangle_T$ are taken such that $\langle\hat{e}\rangle_T=m(T)$, the magnetization of the system at temperature $T$, and $l$ is the order of the spherical harmonic describing the angular dependence of the local anisotropy, i.e., $l=2$ and 4 for uniaxial and cubic systems, respectively. At low temperatures $K(T)/K(0)\approx[m(T)/m(0)]^{l(l+1)/2}$ and near the Curie temperature $T_c$, $K(T)/K(0)\approx[m(T)/m(0)]^l$.

These results can be illustrated straightforwardly in a way which will be helpful for the development of our *ab initio* theory. Consider a classical spin Hamiltonian appropriate to a uniaxial ferromagnet,

$$H=-\frac{1}{2}\sum_{i,j}J_{ij}\hat{e}_i\cdot\hat{e}_j-k\sum_i(\hat{n}_0\cdot\hat{e}_i)^2, \tag{1}$$

where $\hat{e}_i$ describes the orientation of a classical spin at site $i$ and $J_{ij}$ and $k$ are exchange and anisotropy parameters. $\hat{n}_0$ is a unit vector along the magnetic easy axis. A mean field description of the system is given by reference to a Hamiltonian $\Sigma_i\vec{h}\cdot\hat{e}_i$ where the orientation of Weiss field $\vec{h}$, i.e., $\vec{h}=h\hat{n}$, determines the direction of the magnetization of the system and has direction cosines ($\sin\vartheta\cos\varphi$, $\sin\vartheta\sin\varphi$, $\cos\vartheta$). Within this mean field approximation the magnetization $m$ is $\vec{m}(T)=\int\hat{e}P(\hat{e})d\hat{e}$ where the probability of a spin being orientated along $\hat{e}$ is $P(\hat{e})=e^{-\beta h\hat{n}\cdot\hat{e}}/Z_0$ with $Z_0=\int e^{-\beta h\hat{n}\cdot\hat{e}}d\hat{e}$. The free energy difference per site between the system magnetized along two directions $\hat{n}_1$ and $\hat{n}_2$ is

$$K(T)=-\frac{k}{Z_0}\int[(\hat{n}_0\cdot\hat{e})^2e^{-\beta h\hat{n}_1\cdot\hat{e}}-(\hat{n}_0\cdot\hat{e})^2e^{-\beta h\hat{n}_2\cdot\hat{e}}]d\hat{e}. \tag{2}$$

If $\hat{n}_1$ and $\hat{n}_2$ are parallel and perpendicular to the magnetic easy axis $\hat{n}_0$, respectively, then

$$K(T)=-\frac{k}{Z_0}\int g_2(\hat{n}_0\cdot\hat{e})e^{-\beta h\hat{n}_0\cdot\hat{e}}d\hat{e}, \tag{3}$$

where $g_2$ is the Legendre polynomial $[3(\hat{n}_0\cdot\hat{e})^2-1]/2$. As a function of the magnetization $m(T)/m(0)$, $K(T)/K(0)$ varies quadratically near the Curie temperature $T_c$ and cubically at low $T$. The same dependence can be shown for this simple spin model for the rate of variation of magnetic anisotropy with angle $\vartheta$ that the magnetization makes with the system's easy axis, namely the magnetic torque[22] $T_\vartheta=-\partial K/\partial\vartheta$. In order to find out whether a Hamiltonian similar to that in Eq. (1) is appropriate for metallic magnets and if so to set the values of the relevant parameters like $J_{ij}$ and $k$, an *ab initio* approach is necessary. The next section reviews the $T=0$ K limit of this.

## III. *AB INITIO* THEORY OF MAGNETIC ANISOTROPY AT $T=0$ K

Magnetocrystalline anisotropy is caused largely by spin-orbit coupling and receives an *ab initio* description from the relativistic generalization of spin density functional (SDF) theory.[1] Apart from the work by Mryasov *et al.*[14] and ourselves,[13] up to now calculations of the anisotropy

constants $K$ have been suited to $T=0$ K only. Spin-orbit coupling effects are treated perturbatively or with a fully relativistic theory.[4,26] Typically the total energy, or the single-electron contribution to it (if the force theorem is used[27]), is calculated for two or more magnetization directions, $\hat{n}_1$ and $\hat{n}_2$ separately and then the MCA is obtained from the difference, $\Delta E$. $\Delta E$ is typically small ranging from meV to $\mu$eV and high precision in calculating the energies is required. For example, we have used this rationale with a fully relativistic theory to study the MCA of magnetically soft, compositionally disordered binary and ternary component alloys[26,28] and the effect upon it of short-range[4] and long-range chemical order[29] in harder magnets such as CoPt and FePt.

Experimentally, measurements of magnetocrystalline anisotropy constants of magnets can be obtained from torque magnetometry.[22] From similar considerations of magnetic torque, *ab initio* calculations of MCA can be made. There are obvious advantages in that the MCA can be obtained from a single calculation and reliance is not placed on the accurate extraction of a small difference between two energies. In particular, the torque method has been used to good effect by Freeman and co-workers[30] in conjunction with their state-tracking method to study the MCA at $T=0$ K of a range of uniaxial magnets including layered systems.

If the free energy of a material magnetized along a direction specified by $\hat{n}=(\sin\vartheta\cos\varphi,\sin\vartheta\sin\varphi,\cos\vartheta)$ is $F^{(\hat{n})}$, then the torque is

$$\vec{T}^{(\hat{n})} = -\frac{\partial F^{(\hat{n})}}{\partial \hat{n}}. \tag{4}$$

The contribution to the torque from the anisotropic part of $F^{(\hat{n})}$ leads to a direct link between the gap in the spin wave spectrum and the MCA by the solution of the equation[31]

$$\frac{d\hat{n}}{dt} = \gamma(\hat{n} \wedge \vec{T}^{(\hat{n})}), \tag{5}$$

where $\gamma$ is the gyromagnetic ratio. Closely related to $\vec{T}^{(\hat{n})}$ is the variation of $F^{(\hat{n})}$ with respect to $\vartheta$ and $\varphi$, i.e., $T_\vartheta(\vartheta,\varphi)=-\frac{\partial F^{(\hat{n})}}{\partial \vartheta}$ and $T_\varphi(\vartheta,\varphi)=-\frac{\partial F^{(\hat{n})}}{\partial \varphi}$. As shown by Wang *et al.*,[30] for most uniaxial magnets, which are well approximated by a free energy of the form

$$F^{(\hat{n})} = F_{\text{iso}} + K_2 \sin^2\vartheta + K_4 \sin^4\vartheta, \tag{6}$$

(where $K_2$ and $K_4$ and magnetocrystalline anisotropy constants and $F_{\text{iso}}$ is the isotropic part of the free energy), $T_\vartheta(\vartheta=\pi/4,\varphi=0)=-(K_2+K_4)$. This is equal to the MCA, $\Delta F=F^{(1,0,0)}-F^{(0,0,1)}$. For a magnet with cubic symmetry so that

$$F^{(\hat{n})} \approx F_{\text{iso}} + K_1(\sin^4\vartheta\sin^2 2\varphi + \sin^2 2\vartheta), \tag{7}$$

a calculation of $T_\varphi(\vartheta=\pi/2,\varphi=\pi/8)$ gives $-K_1/2$. In this work we present our formalism for the direct calculation of the torque quantities $T_\vartheta(\vartheta,\varphi)$ and $T_\varphi(\vartheta,\varphi)$, and hence the MCA, in which the effects of thermally induced magnetic fluctuations are included so that the temperature dependence is captured.

In our formalism the motion of the electron is described with spin-polarized, relativistic multiple scattering theory. An adaptive mesh algorithm[32] for Brillouin zone integrations is used in the calculations to ensure adequate numerical precision for the MCA to within 0.1 $\mu$eV.[4,26] Since we characterize the thermally induced magnetic fluctuations in terms of disordered local moments, we now go on to describe this picture of finite temperature magnetism.

## IV. METALLIC MAGNETISM AT FINITE TEMPERATURES—DISORDERED LOCAL MOMENTS

In a metallic ferromagnet at $T=0$ K the electronic band structure is spin polarized. With increasing temperature, spin fluctuations are induced which eventually destroy the long-range magnetic order and hence the overall spin polarization of the system's electronic structure. These collective electron modes interact as the temperature is raised and are dependent upon and affect the underlying electronic structure. For many materials the magnetic excitations can be modeled by associating local spin-polarization axes with all lattice sites and the orientations $\{\hat{e}\}$ vary very slowly on the time scale of the electronic motions.[18] These local moment degrees of freedom produce local magnetic fields on the lattice sites which affect the electronic motions and are self-consistently maintained by them. By taking appropriate ensemble averages over the orientational configurations, the system's magnetic properties can be determined.

This disordered local moment picture has been implemented within a multiple-scattering (Korringa-Kohn-Rostoker, KKR)[33–35] formalism using the first principles approach to the problem of itinerant electron magnetism. At no stage does it map the many-electron problem onto an effective Heisenberg model, and yet it deals, quantitatively, with both the ground state and the demise of magnetic long-range order at the Curie temperature in a material-specific, parameter-free manner. It has been used to describe the experimentally observed local exchange splitting and magnetic short-range order in both ultrathin Fe films[36] and bulk Fe, the damped RKKY-like magnetic interactions in the compositionally disordered CuMn spin-glass alloys[37] and the quantitative description of the onset of magnetic order in a range of alloys.[38,39] In combination with the local self-interaction correction (L-SIC)[40] for strong electron correlation effects, it also gives a revealing account of magnetic ordering in rare earths.[41] Other applications of the DLM picture include dilute magnetic semiconductors[42] and actinides.[43] Short-range order of the local moments can be explicitly included by making use of the recently developed KKR-nonlocal-CPA (KKR-NLCPA).[44,45]

We now briefly recap on how this disordered local moment picture is implemented using the KKR-CPA and how a ferromagnetic metal both above and below the Curie temperature can be described. Our main objective in this paper is to explain its relativistic extension and show how this leads to an *ab initio* theory of the temperature dependence of magnetic anisotropy when relativistic effects are explicitly included.

## V. RELATIVISTIC DISORDERED LOCAL MOMENT THEORY

### A. General framework

The nonrelativistic version of the DLM theory has been discussed in detail by Gyorffy *et al.*[19,20] Here we summarize the general framework and concentrate on those aspects which are necessary for a description of magnetic anisotropy. The starting point is the specification of $\Omega^{(\hat{n})}(\{\hat{e}\})$, the generalized electronic grand potential taken from the relativistic extension of spin density functional theory (SDFT).[1,19] It specifies an itinerant electron system constrained such that the local spin polarization axes are configured according to $\{\hat{e}\}=\{\hat{e}_1,\hat{e}_2,\ldots,\hat{e}_N\}$ where $N$ is the number of sites (moments) in the system. For magnetic anisotropy to be described, relativistic effects such as spin-orbit coupling upon the motion of the electrons must be included. This means that orientations of the local moments with respect to a specified direction $\hat{n}$ within the material are relevant. The role of a (classical) local moment Hamiltonian, albeit a highly complicated one, is played by $\Omega^{(\hat{n})}(\{\hat{e}\})$. Note that in the following we do not prejudge the physics by trying to extract an effective spin model from $\Omega^{(\hat{n})}(\{\hat{e}\})$ such as a classical Heisenberg model with a single site anisotropy term.

Consider a ferromagnetic metal magnetized along a direction $\hat{n}$ at a temperature $T$ where the orientational probability distribution is denoted by $P^{(\hat{n})}(\{\hat{e}\})$, and its average

$$\langle \hat{e}_i \rangle = \int \cdots \int \hat{e}_i P^{(\hat{n})}(\{\hat{e}\}) d\hat{e}_1 \cdots d\hat{e}_N = m\hat{n}, \tag{8}$$

is aligned with the magnetization direction $\hat{n}$. The canonical partition function and the probability function are defined as

$$Z^{(\hat{n})} = \int \cdots \int e^{-\beta\Omega^{(\hat{n})}(\{\hat{e}\})} d\hat{e}_1 \cdots d\hat{e}_N, \tag{9}$$

and

$$P^{(\hat{n})}(\{\hat{e}\}) = \frac{e^{-\beta\Omega^{(\hat{n})}(\{\hat{e}\})}}{Z^{(\hat{n})}}, \tag{10}$$

respectively. The thermodynamic free energy which includes the entropy associated with the orientational fluctuations as well as creation of electron-hole pairs, is given by

$$F^{(\hat{n})} = -\frac{1}{\beta} \ln Z^{(\hat{n})}. \tag{11}$$

By choosing a trial Hamiltonian function, $\Omega_0^{(\hat{n})}(\{\hat{e}\})$ with $Z_0^{(\hat{n})}=\int\cdots\int e^{-\beta\Omega_0^{(\hat{n})}(\{\hat{e}\})} d\hat{e}_1\cdots d\hat{e}_N$,

$$P_0^{(\hat{n})}(\{\hat{e}\}) = \frac{e^{-\beta\Omega_0^{(\hat{n})}(\{\hat{e}\})}}{Z_0^{(\hat{n})}} \tag{12}$$

and $F_0^{(\hat{n})}=-\frac{1}{\beta}\ln Z_0^{(\hat{n})}$ the *Feynman-Peierls inequality*[46] implies an upper bound for the free energy, i.e.,

$$F^{(\hat{n})} \leqslant F_0^{(\hat{n})} + \langle \Omega^{(\hat{n})} - \Omega_0^{(\hat{n})} \rangle^0, \tag{13}$$

where the average refers to the probability $P_0^{(\hat{n})}(\{\hat{e}\})$. (In the following we shall omit the superscript 0 from the averages.) By making a mean field approximation and choosing $\Omega_0^{(\hat{n})} \times(\{\hat{e}\})$ to be expressed in terms of *Weiss* fields, $\vec{h}_i^{(\hat{n})}$,

$$\Omega_0^{(\hat{n})}(\{\hat{e}\}) = \sum_i \vec{h}_i^{(\hat{n})} \cdot \hat{e}_i \tag{14}$$

and the best values of $h_i^{(\hat{n})}$ are found to satisfy[19,20]

$$\vec{h}_i^{(\hat{n})} = \int \frac{3}{4\pi} \hat{e}_i \langle \Omega^{(\hat{n})} \rangle_{\hat{e}_i} d\hat{e}_i, \tag{15}$$

where $\langle X \rangle_{\hat{e}_i}$ denotes the average of $X$ with the restriction that the orientation of the moment on site $i$ is fixed as $\hat{e}_i$. (Further details on reaching this result are given in Ref. 19.)

Furthermore,

$$Z_i^{(\hat{n})} = \int \exp(-\beta \vec{h}_i^{(\hat{n})} \cdot \hat{e}_i) d\hat{e}_i \tag{16}$$

$$= \frac{4\pi}{\beta h_i^{(\hat{n})}} \sinh \beta h_i^{(\hat{n})}, \tag{17}$$

where $h_i^{(\hat{n})}=|\vec{h}_i^{(\hat{n})}|$, and the probability distribution is

$$P_i^{(\hat{n})}(\hat{e}_i) = \frac{\beta h_i^{(\hat{n})}}{4\pi \sinh \beta h_i^{(\hat{n})}} \exp(-\beta \vec{h}_i^{(\hat{n})} \cdot \hat{e}_i). \tag{18}$$

The free energy is now given by

$$F^{(\hat{n})} = \langle \Omega^{(\hat{n})} \rangle + \frac{1}{\beta} \sum_i \int P_i^{(\hat{n})}(\hat{e}_i) \ln P_i^{(\hat{n})}(\hat{e}_i) d\hat{e}_i. \tag{19}$$

This is the key expression for our subsequent development of the magnetic anisotropy energy.

Moreover the average alignment of the local moments, proportional to the magnetization, is

$$\vec{m}_i^{(\hat{n})} = \langle \hat{e}_i \rangle = \frac{\beta h_i^{(\hat{n})}}{4\pi \sinh \beta h_i^{(\hat{n})}} \int \hat{e}_i \exp(-\beta \vec{h}_i^{(\hat{n})} \cdot \hat{e}_i) d\hat{e}_i \tag{20}$$

from which $\vec{m}_i^{(\hat{n})}=m_i^{(\hat{n})}\hat{h}_i^{(\hat{n})}$ and

$$m_i^{(\hat{n})} = -\frac{d \ln Z_i^{(\hat{n})}}{d(\beta h_i^{(\hat{n})})} = \frac{1}{\beta h_i^{(\hat{n})}} - \coth \beta h_i^{(\hat{n})} = L(-\beta h_i^{(\hat{n})}) \tag{21}$$

follow, where $L(x)$ is the Langevin function. Since in the ferromagnetic state, $\hat{m}_i=\frac{\vec{m}_i}{m_i}=\hat{n}$ we finally can write the Weiss field, $\vec{h}_i^{(\hat{n})}=h_i^{(\hat{n})}\hat{n}$ as

$$h_i^{(\hat{n})} = \frac{3}{4\pi} \int (\hat{e}_i \cdot \hat{n}) \langle \Omega^{(\hat{n})} \rangle_{\hat{e}_i} d\hat{e}_i. \tag{22}$$

Note that an identical Weiss field $\vec{h}^{(\hat{n})}$ associated with every site corresponds to a description of a ferromagnetic system magnetized along $\hat{n}$ with no reference to an external field.

### B. Averaging with the coherent potential approximation

In order to calculate the restricted average, $\langle \Omega^{(\hat{n})} \rangle_{\hat{e}_i}$, from first principles, as discussed by Gyorffy *et al.*[19] we follow the strategy of the coherent potential approximation (CPA) (Ref. 47) as combined with the KKR multiple scattering theory.[34] The electronic charge density and also the magnetization density, which sets the magnitudes, $\{\mu\}$, of the local moments, are determined from a self-consistent-field (SCF)-KKR-CPA (Ref. 35) calculation. For the systems we discuss in this paper, the magnitudes of the local moments are rather insensitive to the orientations of the local moments surrounding them.[20] We return to this point later.

For a given set of (self-consistent) potentials, electronic charge and local moment magnitudes $\{\mu_i\}$, the orientations of the local moments are accounted for by the similarity transformation of the single-site scattering $t$-matrices,[48]

$$\underline{t}_i(\hat{e}_i) = \underline{R}(\hat{e}_i)\underline{t}_i(\hat{z})\underline{R}(\hat{e}_i)^+, \tag{23}$$

where for a given energy (not labeled explicitly) $\underline{t}_i(\hat{z})$ stands for the $t$-matrix which describes the scattering at a site in the lattice occupied by a potential with an effective magnetic field pointing along the local $z$ axis[49] and $\underline{R}(\hat{e}_i)$ is a unitary representation of the $O$ (3) transformation that rotates the $z$ axis along $\hat{e}_i$. In this work $\underline{t}_i(\hat{z})$ is found by considering the relativistic, spin-polarized scattering of an electron from a central potential with a magnetic field defining the $z$ axis.[49] Thus spin-orbit coupling effects are naturally included.

In principle, for every local moment orientational configuration, $\{\hat{e}_i\}$, the description is needed of the motion of an electron through a lattice of potentials which are spin-polarized according to the prescribed directions $\{\hat{e}_i\}$. Then appropriate ensemble averages for quantities such as $\langle \Omega^{(\hat{n})} \rangle_{\hat{e}_i}$ are taken using the probability distribution $\Pi_i P_i^{(\hat{n})}(\hat{e}_i)$. The CPA was invented to produce a tractable way to carry out these steps. In this approximation a lattice of identical effective potentials is found such that the motion of an electron through this ordered array closely resembles the motion of an electron on the average through the disordered system with fluctuating local moments. The CPA is the requirement that the substitution of a single site of the lattice of these effective potentials by one spin-polarized along a direction $\hat{e}$ produces no further scattering of the electron when the average over $\hat{e}$ is taken. Hence the CPA determines an effective medium through which the motion of an electron mimics the motion of an electron *on the average*. In a system magnetized along a direction $\hat{n}$, the medium is specified by the $t$-matrices, $\underline{t}_{i,c}^{(\hat{n})}$, which satisfy the CPA condition, expressed in scattering theory language,[34]

$$\langle \underline{\tau}_{ii}^{(\hat{n})}(\{\hat{e}\}) \rangle = \int \langle \underline{\tau}_{ii}^{(\hat{n})} \rangle_{\hat{e}_i} P_i^{(\hat{n})}(\hat{e}_i) d\hat{e}_i = \underline{\tau}_{ii,c}^{(\hat{n})}, \tag{24}$$

where the site-diagonal matrices of the multiple scattering path operator[50] are defined as

$$\langle \underline{\tau}_{ii}^{(\hat{n})} \rangle_{\hat{e}_i} = \underline{\tau}_{ii,c}^{(\hat{n})} \underline{D}_i^{(\hat{n})}(\hat{e}_i), \tag{25}$$

$$\underline{D}_i^{(\hat{n})}(\hat{e}_i) = (\underline{1} + \{[\underline{t}_i(\hat{e}_i)]^{-1} - (\underline{t}_{i,c}^{(\hat{n})})^{-1}\}\underline{\tau}_{ii,c}^{(\hat{n})})^{-1}, \tag{26}$$

and

$$\underline{\underline{\tau}}_c^{(\hat{n})} = [(\underline{\underline{t}}_c^{(\hat{n})})^{-1} - \underline{\underline{G}}_0]^{-1}. \tag{27}$$

In the above equation, double underlines denote matrices in site and angular momentum space. $\underline{\underline{t}}_c^{(\hat{n})}$ is diagonal with respect to site indices, while $\underline{\underline{G}}_0$ stands for the matrix of structure constants[32,33] which specify the lattice structure. Equation (24) can be rewritten by introducing the excess scattering matrices,

$$\underline{X}_i^{(\hat{n})}(\hat{e}_i) = (\{(\underline{t}_{i,c}^{(\hat{n})})^{-1} - [\underline{t}_i(\hat{e}_i)]^{-1}\}^{-1} - \underline{\tau}_{ii,c}^{(\hat{n})})^{-1}, \tag{28}$$

in the form

$$\int \underline{X}_i^{(\hat{n})}(\hat{e}_i) P_i^{(\hat{n})}(\hat{e}_i) d\hat{e}_i = \underline{0}. \tag{29}$$

Equation (29) can be solved by iterating together with Eqs. (28) and (27) to obtain the matrices, $\underline{t}_{i,c}^{(\hat{n})}$. The integral in Eq. (29) can be discretized to yield a multicomponent CPA equation which can be solved by the method proposed by Ginatempo and Staunton.[51] Care must be taken, in particular for low temperatures where $P_i^{(\hat{n})}(\hat{e}_i)$ is a sharply structured function, to include a large number and/or an adaptive sampling of the grid points.

### C. Calculation of the Weiss field

In the spirit of the *magnetic force theorem*[27] we shall consider only the single-particle energy (band energy) part of the SDFT grand potential as an effective local moment Hamiltonian in Eq. (22),

$$\Omega^{(\hat{n})}(\{\hat{e}\}) \simeq -\int d\varepsilon f_{\mathrm{FD}}(\varepsilon;\nu^{(\hat{n})}) N^{(\hat{n})}(\varepsilon;\{\hat{e}\}), \tag{30}$$

where $\nu^{(\hat{n})}$ is the chemical potential, $f_{\mathrm{FD}}(\varepsilon;\nu^{(\hat{n})})$ is the Fermi-Dirac distribution, and $N^{(\hat{n})}(\varepsilon;\{\hat{e}\})$ denotes the integrated density of states for the orientational configuration, $\{\hat{e}\}$.

The Lloyd formula[52] provides an explicit expression for $N^{(\hat{n})}(\varepsilon;\{\hat{e}\})$,

$$N^{(\hat{n})}(\varepsilon;\{\hat{e}\}) = N_0(\varepsilon) - \frac{1}{\pi} \mathrm{Im} \ln \det[\underline{\underline{t}}^{(\hat{n})}(\varepsilon;\{\hat{e}\})^{-1} - \underline{\underline{G}}_0(\varepsilon)] \tag{31}$$

with $N_0(\varepsilon)$ being the integrated DOS of the free particles. As shown in Ref. 53 the configurationally averaged integrated density of states given by the CPA can be written in the following way:

$$\langle N^{(\hat{n})}(\varepsilon;\{\hat{e}\}) \rangle = N_0(\varepsilon) - \frac{1}{\pi} \mathrm{Im} \ln \det[\underline{\underline{t}}_c^{(\hat{n})}(\varepsilon)^{-1} - \underline{\underline{G}}_0(\varepsilon)] - \frac{1}{\pi} \mathrm{Im} \sum_i \langle \ln \det \underline{M}_i^{(\hat{n})}(\varepsilon;\hat{e}_i) \rangle, \tag{32}$$

where $\underline{M}_i^{(\hat{n})}(\varepsilon;\hat{e}_i) = \underline{D}_i^{(\hat{n})}(\varepsilon,\hat{e}_i)^{-1}$, defined in Eq. (26). A useful property of this expression is that it is stationary with respect

to changes in the $t$-matrices, $\underline{\underline{t}}_c^{(\hat{n})}(\varepsilon)$, which determine the effective CPA medium. Indeed this stationarity condition can be shown to be another way of expressing the CPA condition.[53] We will use this shortly in our derivation of a robust expression for the calculation of the MCA.

The partially averaged electronic grand potential is given by

$$\langle \Omega^{(\hat{n})} \rangle_{\hat{e}_i} = -\int d\varepsilon f_{\mathrm{FD}}(\varepsilon;\nu^{(\hat{n})}) N_c^{(\hat{n})}(\varepsilon) + \frac{1}{\pi}\int d\varepsilon f_{\mathrm{FD}}(\varepsilon;\nu^{(\hat{n})}) \mathrm{Im} \ln \det \underline{M}_i^{(\hat{n})}(\varepsilon;\hat{e}_i) + \sum_{j\neq i}\frac{1}{\pi}\int d\varepsilon f_{\mathrm{FD}}(\varepsilon;\nu^{(\hat{n})}) \mathrm{Im}\langle \ln \det \underline{M}_j^{(\hat{n})}(\varepsilon;\hat{e}_j)\rangle, \tag{33}$$

where $N_c^{(\hat{n})}(\varepsilon) = \frac{1}{\pi}\,\mathrm{Im}\int \ln \det(\underline{\underline{t}}_c^{(\hat{n})}(\varepsilon)^{-1} - \underline{\underline{G}}_0(\mathbf{k},\varepsilon))d\mathbf{k}$ and the Weiss field, $h_i^{(\hat{n})}$, can be expressed, using Eq. (22), as

$$h_i^{(\hat{n})} = \frac{3}{4\pi}\int (\hat{e}_i\cdot\hat{n})\left(\int d\varepsilon f_{\mathrm{FD}}(\varepsilon;\nu^{(\hat{n})})\frac{1}{\pi}\,\mathrm{Im}\ln\det \underline{M}_i^{(\hat{n})} \times(\varepsilon;\hat{e}_i)\right) d\hat{e}_i. \tag{34}$$

The solution of Eqs. (34) and (20) produces the variation of the magnetization $m_i^{(\hat{n})}$ with temperature $T$ with $m_i^{(\hat{n})}$ going to zero at $T=T_c^{(\hat{n})}$. When relativistic effects are included, the magnetization direction $\hat{n}$ for which $T_c^{(\hat{n})}$ is highest indicates the easy direction for the onset of magnetic order. We can define a temperature range $\Delta T_{\mathrm{aniso}} = T_c^{(\hat{n}_e)} - T_c^{(\hat{n}_h)}$ where $\hat{n}_e$ and $\hat{n}_h$ are the system's high temperature easy and hard directions, respectively, which is related to the magnetic anisotropy of the system at lower temperatures. Indeed an adaptation of this approach to systems such as thin films in combination with $T=0$ K calculations may be useful in understanding temperature-induced spin reorientation transitions.[54]

## VI. THEORETICAL FORMALISM FOR THE MAGNETIC ANISOTROPY *AB INITIO*

In the ferromagnetic state, at temperatures more than $\Delta T_{\mathrm{aniso}}$ below the Curie temperature, the magnetic anisotropy is given by the difference between the free energies, $F^{(\hat{n})}$, for two different magnetization directions, $\hat{n}_1$, $\hat{n}_2$, but the same magnetization $m$ and therefore the same values of the products of the Weiss field magnitudes with $\beta$, i.e., $\beta h_i^{(\hat{n}_1)} = \beta h_i^{(\hat{n}_2)}$. Within our DLM theory this means that the single site entropy terms in Eq. (19) for each magnetization direction cancel when the difference is taken and the magnetic anisotropy energy MCA can be written

$$\Delta F(\hat{n}_1,\hat{n}_2) = \langle \Omega^{(\hat{n}_1)}\rangle - \langle \Omega^{(\hat{n}_2)}\rangle. \tag{35}$$

This becomes $\Delta F(\hat{n}_1,\hat{n}_2) \approx -\int d\varepsilon f_{\mathrm{FD}}(\varepsilon;\nu^{(\hat{n}_1)})[\langle N^{(\hat{n}_1)}(\varepsilon)\rangle - \langle N^{(\hat{n}_2)}(\varepsilon)\rangle]$ where a small approximation is made through the use of the one chemical potential $\nu^{(\hat{n}_1)}$. Using Eq. (32) this can be written explicitly as

$$\begin{aligned}\Delta F(\hat{n}_1,\hat{n}_2) = &-\int d\varepsilon f_{\mathrm{FD}}(\varepsilon;\nu^{(\hat{n}_1)})\frac{\mathrm{Im}}{\pi}\int \ln\det\{\underline{1} + [\underline{\underline{t}}_c^{(\hat{n}_1)}(\varepsilon)^{-1} \\ &- \underline{\underline{t}}_c^{(\hat{n}_2)}(\varepsilon)^{-1}]\underline{\tau}_c^{(\hat{n}_2)}(\varepsilon,\mathbf{k})\}d\mathbf{k} \\ &- \sum_i \int d\varepsilon f_{\mathrm{FD}}(\varepsilon;\nu^{(\hat{n}_1)})\frac{\mathrm{Im}}{\pi}\int [P_i^{(\hat{n}_1)} \\ &\times(\hat{e}_i)\ln\det \underline{M}_i^{(\hat{n}_1)}(\varepsilon;\hat{e}_i) - P_i^{(\hat{n}_2)}(\hat{e}_i)\ln\det \underline{M}_i^{(\hat{n}_2)} \\ &\times(\varepsilon;\hat{e}_i)]d\hat{e}_i,\end{aligned} \tag{36}$$

where $\underline{\tau}_c^{(\hat{n}_2)}(\varepsilon,\mathbf{k})$ is the lattice Fourier transform of the inverse of the KKR matrix $[\underline{\underline{t}}_c^{(\hat{n}_2)}(\varepsilon)^{-1} - \underline{\underline{G}}_0(\varepsilon)]$. As well as ensuring that the Brillouin zone integration over the wave vector $\mathbf{k}$ in the above equation is accomplished with high numerical precision,[4,26] care must also be taken to establish accurately the two CPA media describing the system magnetized along the two directions, $\hat{n}_1$ and $\hat{n}_2$. Equation (29) must be solved to high precision in each case. These steps were successfully taken and tested for our first application on $L1_0$-FePt.[13] We have found however that a less computationally demanding scheme for extracting the temperature dependence of the magnetic anisotropy can be derived by consideration of the magnetic torque. It is sufficiently robust numerically to be applicable to a range of magnetic materials, whether hard or soft magnetically and in bulk, film and nanoparticulate form.

## VII. A TORQUE-BASED FORMULA FOR THE MAGNETIC ANISOTROPY

We return again to Eq. (19) for the expression for the free energy $F^{(\hat{n})}$ of a system magnetized along a direction $\hat{n}=(\sin\vartheta\cos\varphi, \sin\vartheta\sin\varphi, \cos\vartheta)$ and consider how it varies with change in magnetization angles $\vartheta$ and $\varphi$, i.e., $T_\vartheta = -\frac{\partial F^{(\hat{n})}}{\partial\vartheta}$, $T_\varphi = -\frac{\partial F^{(\hat{n})}}{\partial\varphi}$. Since the single site entropy term in Eq. (19) is invariant with respect to the angular variations we can write

$$T_{\vartheta(\varphi)} = -\frac{\partial}{\partial\vartheta(\varphi)}\left(\sum_i \int P_i^{(\hat{n})}(\hat{e}_i)\langle\Omega^{(\hat{n})}\rangle_{\hat{e}_i} d\hat{e}_i\right). \tag{37}$$

By using Eqs. (32) and (33), together with the stationarity of the CPA integrated density of states to variations of the CPA effective medium, we can write directly

$$T_{\vartheta(\varphi)} = -\frac{\mathrm{Im}}{\pi}\int d\varepsilon f_{\mathrm{FD}}(\varepsilon;\nu^{(\hat{n})})\left(\sum_i \int \frac{\partial P_i^{(\hat{n})}(\hat{e}_i)}{\partial\vartheta(\varphi)}\ln\det \underline{M}_i^{(\hat{n})} \times(\varepsilon;\hat{e}_i)d\hat{e}_i\right). \tag{38}$$

According to the form of $P_i^{(\hat{n})}(\hat{e}_i)$ given in Eq. (18) the principal expression for the magnetic torque at finite temperature is thus

$$T_{\vartheta(\varphi)} = \frac{\mathrm{Im}}{\pi} \int d\varepsilon f_{\mathrm{FD}}(\varepsilon;\nu^{(\hat{n})}) \Bigg[ \sum_i \int \beta h_i P_i^{(\hat{n})}(\hat{e}_i) \times \left( \frac{\partial \hat{n}}{\partial \vartheta(\varphi)} \cdot \hat{e}_i \right) \ln \det \underline{M}_i^{(\hat{n})}(\varepsilon;\hat{e}_i) d\hat{e}_i \Bigg]. \quad (39)$$

In the Appendix we derive $T_{\vartheta(\varphi)}$ for a magnet at $T=0$ K and show that this is equivalent to Eq. (38) for the limit $\beta h \to \infty$, i.e., when $T \to 0$ K.

## VIII. THE CALCULATION OF THE TEMPERATURE DEPENDENCE OF THE MAGNETIZATION, $M(T)$, AND THE $M(T)$ DEPENDENCE OF THE MAGNETIC ANISOTROPY

In a first-principles implementation of the DLM picture, the averaging over the orientational configurations of the local moments is performed using techniques adopted from the theory of random metallic alloys.[19,35] Over the past 20 years, the paramagnetic state, onset of magnetic order and transition temperatures of many systems have been successfully described. All applications to date, apart from our earlier study of FePt (Ref. 13) and the cases described in this paper, have, however, neglected relativistic effects and have been devoted to the paramagnetic state where the symmetry turns the calculation into a binary alloy-type one with one-half the moments oriented along a direction and the rest antiparallel. Once relativistic effects are included and/or the ferromagnetic state is considered, this simplicity is lost and, as is shown above, the continuous probability distribution, $P_i^{(\hat{n})} \times (\hat{e}_i)$, must be sampled for a fine mesh of angles and the averages with the probability distribution performed numerically. [Careful checks must be made to ensure that the sampling of $P_i^{(\hat{n})}(\hat{e}_i)$ is sufficient—in our calculations up to 40 000 values are used.] Of course, in the paramagnetic state $P_i^{(\hat{n})}(\hat{e}_i) = \frac{1}{4\pi}$ so that a local moment on a site has an equal probability in pointing in any direction $\hat{e}_i$.

The local moments change their orientations, $\{\hat{e}_i\}$, on a time scale $\tau$ long in comparison with the time taken for electrons to hop from site to site. Meanwhile their magnitudes fluctuate rapidly on this fast electronic time scale which means that over times $\tau$, the magnetization on a site is equal to $\mu_i \hat{e}_i$. As a consequence of the itinerant nature of the electrons, the magnitude $\mu_i$ depends on the orientations of the local moments on surrounding sites, i.e., $\mu_i = \mu_i(\{\hat{e}_l\})$. In the DLM theory described above, $\mu_i = \langle \mu_i(\{\hat{e}\}) \rangle_{\hat{e}_i}$, so that the size of the local moment on a site is taken from electronic charge density spin-polarized along $\hat{e}_i$ and integrated over the site. An average is taken over the orientations $\{\hat{e}\}$ on surrounding sites and the local charge and magnetization densities are calculated self-consistently from a generalized SDFT formalism and SCF-KKR-CPA techniques.

Being a local mean field theory, the principal failure of the DLM to date is that it does not give an adequate description of local moment formation in Ni rich systems because it cannot allow for the effects of correlations among the orientations of the local moments over small neighborhoods of atomic sites. (In principle this shortcoming is now addressable using the newly developed SCF-KKR-NLCPA method.[44,45]) In this paper however we will focus entirely on good local moment systems where the sizes of the moments are rather insensitive to their orientational environments. In these cases, for example, the self-consistently determined local moments of the paramagnetic DLM state differ little from the magnetization per site obtained for the ferromagnetic state. For example, in paramagnetic DLM $L1_0$-FePd, a local moment of $2.98\mu_B$ is set up on each Fe site while no moment forms on the Pd sites. For the same lattice spacings ($c=0.381$ nm, $c/a=1$—note we have neglected the deviation of $c/a$ from ideal found experimentally) we find that, for the completely ferromagnetically ordered state of FePd at $T=0$ K, the magnetization per Fe site is $2.96\mu_B$ and a small magnetization of $0.32\mu_B$ is associated with the Pd sites. Likewise, the $Fe_{50}Pt_{50}$ fcc disordered alloy has local moments of $2.92\mu_B$ on the Fe sites in the paramagnetic state while the ferromagnetic state has magnetization of $2.93\mu_B$ and $0.22\mu_B$ on each Fe and Pt site, respectively ($a=0.385$ nm). We can therefore safely use the self-consistently generated effective potentials and magnetic fields for the paramagnetic DLM state along with the charge and magnetization densities for calculations for the ferromagnetic state below $T_c$.

Our calculational method therefore is comprised of the following steps:

(1) Perform self-consistent scalar-relativistic DLM calculations for the paramagnetic state, $T > T_c$, to form effective potentials and magnetic fields from the local charge and magnetization densities [using typically the local spin density approximation (LSDA)]. Using relativistic, spin-polarized scattering theory find the single-site $t$-matrices, $\underline{t}_i^{(\hat{n})}(\hat{z})$ from these effective potentials and magnetic fields.

(2) Carry out a fully relativistic DLM calculation. For a given temperature and orientation, $\hat{n} = (\sin\vartheta\cos\varphi, \sin\vartheta\sin\varphi, \cos\vartheta)$ determine the $h_i^{(\hat{n})}$'s [and also the chemical potential $\nu^{(\hat{n})}$ from Eq. (32)] self-consistently:

(a) for a set of $\lambda_i = \beta h_i^{(\hat{n})}$ determine the $\underline{t}_{i,c}^{(\hat{n})}$ by solving the CPA condition, Eq. (29);

(b) calculate new Weiss fields, Eq. (34);

(c) repeat steps (2) (a) and (b) until convergence. [For a system where there is a single local moment per unit cell, this iterative procedure can be circumvented. A series of values of $\lambda(=\beta h^{(\hat{n})})$ is picked to set the probabilities, $P^{(\hat{n})}(\hat{e}_i)$ (and magnetizations $\vec{m} = \langle \hat{e} \rangle$, $m = |\vec{m}|$). The Weiss field $h^{(\hat{n})}$ is then calculated from (34) and the ratio of $h^{\hat{n}}$ to $\lambda$ then uniquely determines the temperature $T$ for each of the initially chosen values of $\lambda$ and hence the temperature dependence of the magnetization.]

(3) Calculate the torque, $T_{\vartheta(\varphi)}$ from Eq. (39) to give the magnetic anisotropy and also average alignment of the local moments, $\vec{m}_i^{(\hat{n})}(T)$, proportional to the total magnetization, $\mu_i \vec{m}_i$, from Eq. (20).

(4) Repeat steps (2) and (3) for a different direction, $\hat{n}'$ if necessary.

[On a technical point: all integrals over energy $\frac{\mathrm{Im}}{\pi} \int d\varepsilon f_{\mathrm{FD}}(\varepsilon;\nu^{(\hat{n})}) \cdots$ are carried out via a suitable contour in the complex energy plane and a summation over Matsubara

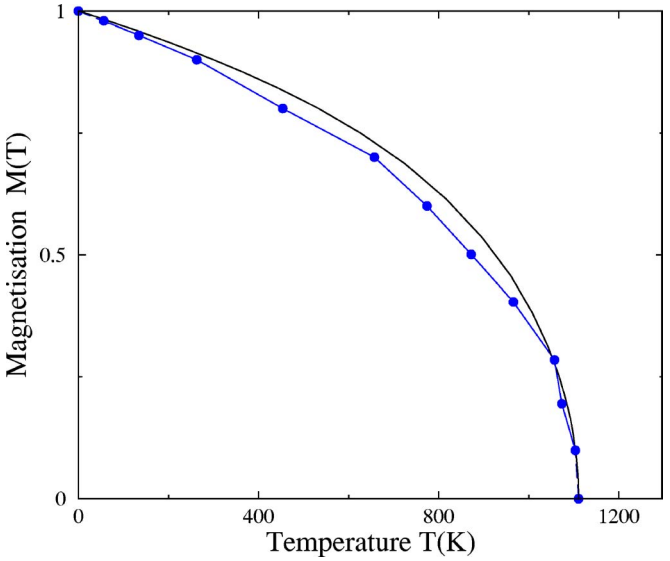


FIG. 1. (Color online) The magnetization of FePt versus temperature. The filled circles refer to a magnetization along $\hat{n}=(1,0,1)$. $T_c$ is at 1105 K with the easy axis, (0,0,1). The full line shows the mean field approximation to a classical Heisenberg model for comparison.

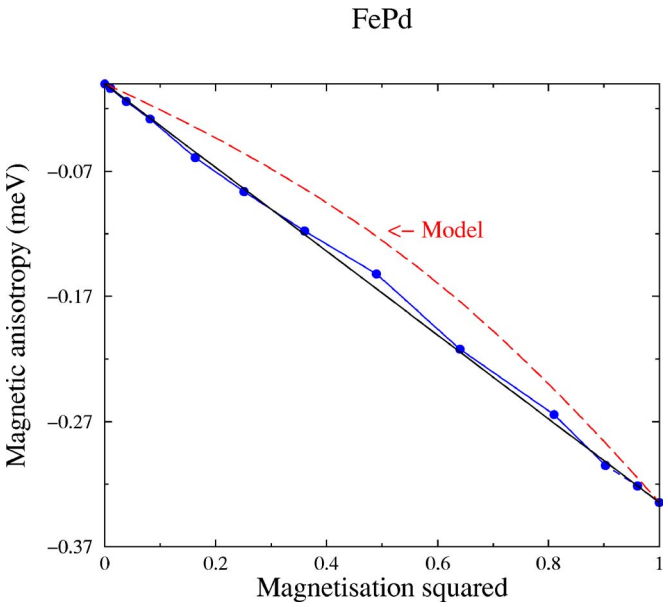


FIG. 2. (Color online) The magnetic anisotropy of FePd as a function of the square of magnetization. The filled circles show the calculations from the *ab initio* theory, the full line $K_0[m(T)/m(0)]^2$, and the dashed line the single-ion model function $K_0\langle g_2(\hat{e})\rangle_T/\langle g_2(\hat{e})\rangle_0$ with $K_0=-0.335$ meV.

frequencies.[55] We use a simple box contour which encloses Matsubara frequencies up to $\approx 10$ eV/$\hbar$.]

In the following examples for the uniaxial ferromagnets FePt and FePd, we have carried through steps (1) to (4) for $\vartheta_1=\frac{\pi}{4}, \varphi_1=0$ where $T_\vartheta=-(K_2+K_4)$ $(T_\varphi=0)$ and also for $\vartheta_2=\frac{\pi}{3}$, $\varphi_2=0$ where $T_\vartheta=-\frac{\sqrt{3}}{2}\left(K_2+\frac{3}{2}K_4\right)$ $(T_\varphi=0)$. For the cubic magnet disordered FePt we use $\vartheta_1=\frac{\pi}{4}$, $\varphi_1=0$ as a numerical check, where both $T_\vartheta$ and $T_\varphi$ should be zero, and $\vartheta_2=\frac{\pi}{2}$, $\varphi_2=\frac{\pi}{8}$ where $T_\vartheta=0$ and $T_\varphi=-\frac{K_1}{2}$.

## IX. UNIAXIAL MAGNETIC ANISOTROPY—FERROMAGNETS WITH TETRAGONAL CRYSTAL SYMMETRY

Our first case study in this paper is $L1_0$-FePd and the trends we find are very similar to those we found for $L1_0$-FePt.[13] Figure 1 shows the dependence of the magnetization upon temperature. In this mean field approximation we find a Curie temperature of 1105 K in reasonable agreement with the experimental value of 723 K.[56] (An Onsager cavity field technique could be used to improve this estimate, see Ref. 20, without affecting the quality of the following results for $K$.) Although the shortcomings of the mean field approach do not produce the spin wave $T^{3/2}$ behavior at low temperatures, the easy axis for the onset of magnetic order is deduced, $\hat{n}=(0,0,1)$ perpendicular to the layering of the Fe and Pd atoms (not shown in the figure) and it corresponds to that found at lower temperatures both experimentally[57] and in all theoretical ($T=0$ K) calculations.[58] Figure 2 shows the magnetic anisotropy energy, $\Delta F[(0,0,1),(1,0,0)]=-(K_2+K_4)$ versus the square of the magnetization. The same linear relationship that we found for FePt (Ref. 13) is evident, a clear consequence of the itinerant nature of the magnetism is this system. This magnetization dependence differs significantly from that produced by the single ion model, also shown in the figure. At $T=0$ K, $K_2+K_4$ is 0.335 meV is in fair agreement with the value of 0.373 meV inferred from low temperature measurements on well ordered samples[57] (as with FePt, $K$ decreases significantly if the degree of long-range chemical order is reduced). The value is also in line with values of 0.1 to 0.5 meV found by other *ab initio* approaches.[58] From $T_\vartheta$ for both $\vartheta=\frac{\pi}{4}$, $\varphi=0$ and $\vartheta=\frac{\pi}{3}$, $\varphi=0$ the magnitudes of the MCA constants $K_2$ and $K_4$ are extracted and shown in Fig. 3. The dominance of $K_2$ is obvious but it is also clear that the $m^2$ dependence is followed closely by the total anisotropy, $K_2+K_4$, and only approximately by the leading constant $K_2$. It is interesting to note that an anisotropic classical Heisenberg model leads to similar $m$ dependence to $K$ if treated within a mean field approach. To illustrate this point we show in Fig. 4 the results of mean field calculations of $K$ for a model with both single-ion and anisotropic nearest-neighbor exchange, i.e., where the following Hamiltonian is appropriate:

$$H=-\frac{1}{2}\sum_{i,j}\left[J^{\parallel}(e_{x,i}e_{x,j}+e_{y,i}e_{y,j})+J^{\perp}e_{z,i}e_{z,j}\right]-k\sum_i (e_{z,i})^2. \tag{40}$$

The full curve shows the single ion model results for the limit $J^{\parallel}=J^{\perp}$, which are also shown in Fig. 3. At low $T$ as $m(T)\to 1$, $K(T)/K(0)$ has the familiar $m^{l(l+1)/2}$ form with $l=1$ for a uniaxial magnet. By introducing a small difference between $J^{\parallel}$ and $J^{\perp}$, so that $J^{\perp}-J^{\parallel}=0.01J^{\perp}$, $K(T)/K(0)$ varies as $m^2$.

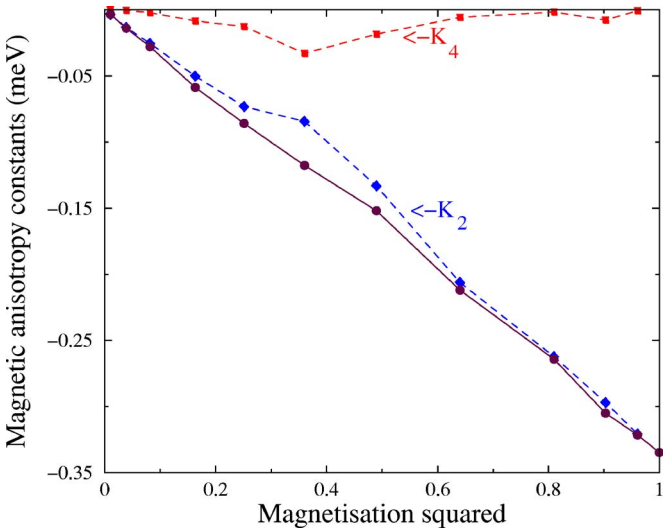


FIG. 3. (Color online) The magnetic anisotropy constants $K_2$, $K_4$ of FePd as a function of the square of magnetization. The filled circles and full line show the calculations from the *ab initio* theory of the sum, the dashed line with filled diamonds describes $K_2$ and the dotted line with squares shows $K_4$.

To our knowledge experimental studies of the thermal variation of $K$ over a wide range of values of $m$ has not been undertaken for $L1_0$-FePd. Recently, however, Shima *et al.*[60] examined the variation of $K$ over a range of temperatures where $m(T)$ varies from 1 to 0.94. They prepared a bulk $Fe_{48}Pd_{52}$ single crystal in a single variant state by heat treatment under compressive stress and deduced that the $L1_0$ order parameter was roughly 0.8. They found the magnetic easy axis to be aligned with the $c$ axis and $K(T)$ to decrease with increasing $T$ and found the data best fit to $K(T)/K(0) \sim m(T)^{3.3}$. Although the easy axis and magnitude of $K(0)$ (0.44 meV) agrees quite well with our results, clearly the value of the extracted power of $m$ for this range of values of $m$ does not and is closer to that from the single ion model. The experimental data were fit assuming a value of $T_c \approx 650$ K where $K(T) \rightarrow 0$ which is somewhat lower than that of 723 K measured elsewhere.[56] This suggests that for $m < 0.9$ the variation of $K(T)$ could follow a dependence on $m$ closer to our *ab initio* theory. Measurements using the same techniques on an $L1_0$-$Fe_{60}Pt_{40}$ single crystal by the same group[61] found $K(T)/K(0) \sim m(T)^n$ where $n > 4$ for $m$ near 1 and consequently showing a qualitative difference from the measurements on $L1_0$-FePt by Okamoto *et al.*[17] who found $K(T)/K(0) \sim m(T)^2$. This was explained in part by the thermal variation of the $c/a$ ratio owing to thermal expansion that occurs in the single variant structures of Ref. 61. In our work, as well as assuming perfect $L1_0$ order, we have fixed $c/a$ at the ideal value of 1 for all values of $m$ and so have not included this thermal expansion effect.

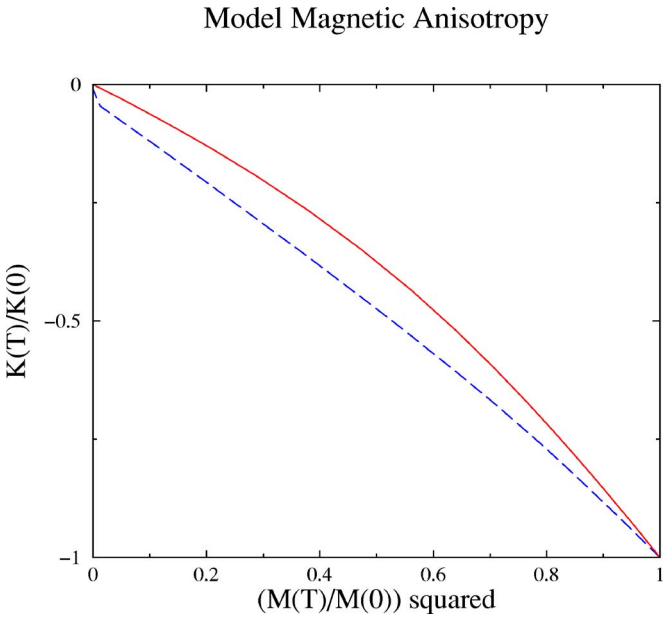


FIG. 4. (Color online) The magnetic anisotropy energy $K$ calculated in a mean field approximation for a model of a uniaxial magnet which has both anisotropic exchange and single ion anisotropy. The full line shows results with single ion anisotropy only, $k = 0.002 J^{\perp}$ and $J^{\perp} - J^{\parallel} = 0$. The dashed line shows results for the same $k$ and $J^{\perp} - J^{\parallel} = 0.01 J^{\perp}$.

## X. CUBIC MAGNETIC ANISOTROPY—THE fcc $Fe_{50}Pt_{50}$ SOLID SOLUTION

Crystal structure is known to have a profound effect upon the magnetic anisotropy. Magnetic anisotropy within a single ion anisotropy model decreases according to $m^{l(l+1)/2}$ at low $T$ ($m \approx 1$) and proportional to $m^l$ for small $m$ at higher $T$. For materials with tetragonal symmetry, $l=2$ as shown in Fig. 2. On this basis a cubic magnet's $K$ should possess an $m$ dependence where $l=4$, i.e., $m^{10}$ at low $T$ and $m^4$ at higher $T$. In this section we show our results for the itinerant magnet, compositionally disordered $Fe_{50}Pt_{50}$ where the lattice sites of the fcc lattice are occupied at random by either Fe or Pt atoms. The cubic symmetry causes this alloy to be magnetically very soft whereas ordering into a tetragonal $L1_0$ structure of Fe-rich layers stacked alternately with Pt layers along the (1,0,0) direction causes a significant increase of $K$ and the alloy becomes a uniaxial ferromagnet. Okamoto *et al.*[17] have measured $K$ of FePt carefully as a function of compositional order and the trend, for $T=0$ K, has been successfully reproduced in *ab initio* calculations.[29,59] The experimental data also shows that rate of decrease of $K$ with increasing $T$ steepens as the degree of long range order reduces from the complete order of the $L1_0$-FePt alloy to zero for $Fe_{50}Pt_{50}$. In this section we show the microscopic origin of this feature by describing our calculations of the magnetization dependence of disordered $Fe_{50}Pt_{50}$ and comparing them with our earlier ones for $L1_0$-FePt.

As with our other calculations the magnetization of the disordered $Fe_{50}Pt_{50}$ alloy follows a similar $T$ dependence to that of a mean field treatment of a classical Heisenberg model. We find a Curie temperature of 1085 K, again a mean field value which is in reasonable agreement with the experimental value of 750 K.[17] Figure 5 shows our calculations of the magnetization dependence of the leading magnetic anisotropy constant $K_1$ [Eq. (7)]. At $T=0$ K, $\Delta F[(0,0,1),(1,1,1)] = -K_1/3$ is just 2.8 $\mu$eV ($\pm 0.1$ $\mu$eV),

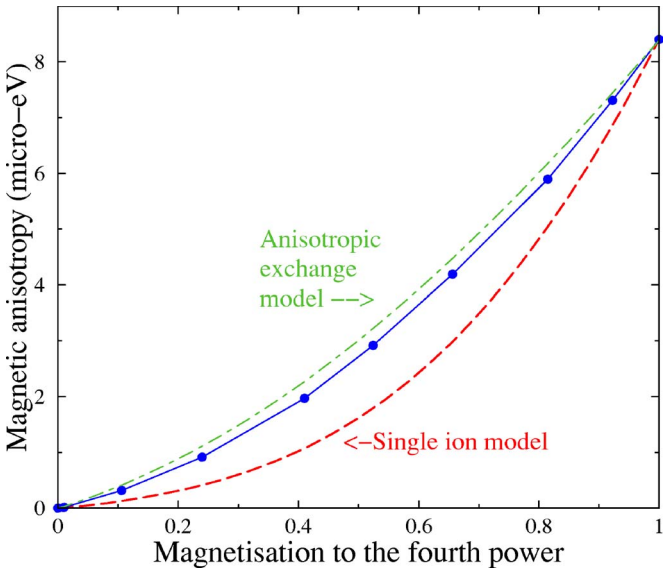


FIG. 5. (Color online) The magnetic anisotropy constant $K_1$ of the cubic magnet $Fe_{50}Pt_{50}$ as a function of the fourth power of the magnetization, $m^4$. The filled circles show the calculations from the *ab initio* theory, the dashed line from the single-ion anisotropy model $k\Sigma_i(e_{x,i}^2e_{y,i}^2+e_{y,i}^2e_{z,i}^2+e_{z,i}^2e_{y,i}^2)$ and the dotted-dashed line from the anisotropic exchange two ion model $\frac{1}{2}\Delta J\Sigma_{i,j}(e_{x,i}^2e_{y,j}^2+e_{y,i}^2e_{z,j}^2+e_{z,i}^2e_{x,j}^2)$ with $k=\Delta J=8.4$ $\mu$eV.

some three orders of magnitude smaller than the uniaxial MCA ($K_2+K_4$) we find for its $L1_0$-ordered counterpart.[13] Despite this small value we find that our method is robust enough to follow the magnetization and $T$ dependence of $K_1$. $K_1$ is determined from a calculation of $T_\varphi$ where for $\vartheta=\pi/2$ and $\varphi=\pi/8$ it equals $K_1/2$. The cubic symmetry of $Fe_{50}Pt_{50}$ causes $K_1$ to decrease much more rapidly with $m$ than the $m^2$ dependence shown by its tetragonal $L1_0$-FePt counterpart. Figure 5 depicts $K_1$ versus the fourth power of the magnetization. At low $T$ $K_1$ varies approximately as $m^7$ whereas this dependence becomes $m^4$ for smaller $m$ and higher $T$. Figure 5 also shows the behavior of both the single ion anisotropy model, $k\Sigma_i(e_{x,i}^2e_{y,i}^2+e_{y,i}^2e_{z,i}^2+e_{z,i}^2e_{y,i}^2)$, and an anisotropic exchange or two ion model, $\frac{1}{2}\Delta J\Sigma_{i,j}(e_{x,i}^2e_{y,j}^2+e_{y,i}^2e_{z,j}^2+e_{z,i}^2e_{x,j}^2)$, for a cubic system for comparison. As with the uniaxial metallic magnets already investigated, the *ab initio* R-DLM results follow the same power law dependence on $m$ for small $m$ as both models which is $m^4$ in this cubic case. For $m\rightarrow 1$, the power increases significantly to $m^7$ for the *ab initio* results, $m^{10}$ for the single ion model, $m^6$ for the two ion model. As in the case of the uniaxial FePd magnet, Fig. 4, the *ab initio* results can be understood from an interpretation based on a model with predominantly anisotropic exchange. We note that the high power law decrease of cubic anisotropy with magnetization found in both our *ab initio* calculations and in the single ion anisotropy models has been observed experimentally in several cubic metallic magnets, e.g., bcc Fe (Ref. 62) and thick Fe films sandwiched between $W$ slabs.[63]

## XI. CONCLUSIONS

We have shown that by including relativistic effects such as spin-orbit coupling into the disordered local moment theory of finite temperature magnetism, the microscopic origin for the temperature dependence of magnetic anisotropy of metallic magnets can be obtained. Magnetic anisotropy is determined via consideration of magnetic torque expressed within a multiple-scattering formalism for the electronic motion. For uniaxial metallic magnets with tetragonal crystal symmetry, $L1_0$-FePt and FePd, we find $K$ to vary with the square of the overall magnetization, $m(T)$. This is at odds with what an analysis based on a single ion anisotropy model would find but in agreement with experimental measurements for FePt. An interpretation in terms of an anisotropic two ion model explains this behavior.[14] We suggest that this $m^2$ behavior is typical for high $T_c$ transition metal alloys ordered into a tetragonal structure when lattice expansion effects are neglected. We find the first anisotropy coefficient, $K_2$ to be dominant. We have also investigated the magnetic anisotropy of metallic magnets with cubic crystal symmetry which are very soft magnetically. In the example of the fcc substitutional alloy, $Fe_{50}Pt_{50}$, the leading constant $K_1$ decreases according to $m^n$ where $n$ ranges between 7 and 4 as the temperature is increased. This behavior also differs from that of a simple single ion model and, as with the uniaxial magnets, is closer to that of a two ion model. It shows how the fall off of MCA with magnetization steepens dramatically when the symmetry of the system is increased from tetragonal to cubic as found experimentally. Application of this R-DLM theory of magnetism at finite temperature has been confined here to bulk crystalline systems. It also, however, has particular relevance for thin film and nanostructured metallic magnets[64–66] where it can be used to uncover temperature-induced reorientation transitions. For example, Buruzs *et al.*[54] have recently applied the theory to Fe and Co monolayers on Cu(111). Future possible applications also include the study of the temperature dependence of magnetostriction, the design of high permeability materials and magnetotransport phenomena in spintronics.

## ACKNOWLEDGMENTS

The authors acknowledge support from the EPSRC (U.K), the Centre for Scientific Computing at the University of Warwick, the Hungarian National Science Foundation (OKTA T046267) and to the Center for Computational Materials Science (Contracts Nos. FWF W004 and GZ 45.547).

## APPENDIX: TORQUE FOR $T\rightarrow 0$ K

Concerning the MCA of a ferromagnet at $T=0$ K, the relevant part of the total energy is

$$F^{(\hat{n})} = -\int d\varepsilon f_{\mathrm{FD}}(\varepsilon;\nu^{(\hat{n})})N^{(\hat{n})}(\varepsilon), \tag{A1}$$

where $N^{(\hat{n})}(\varepsilon)$ is the integrated density of states,

$$N^{(\hat{n})}(\varepsilon) = N_0(\varepsilon) - \frac{1}{\pi}\,\mathrm{Im}\,\ln\det[\underline{\underline{t}}(\hat{n};\varepsilon)^{-1} - \underline{\underline{G}}_0(\varepsilon)], \tag{A2}$$

and the single site $t$-matrix is

$$\underline{t}_i(\hat{n};\varepsilon) = \underline{R}(\hat{n})\underline{t}_i(\hat{z};\varepsilon)\underline{R}(\hat{n})^+. \tag{A3}$$

Now $\underline{R}(\hat{n})=\exp i\alpha_{\hat{m}}(\hat{m}\cdot\vec{\underline{J}})$ where $\alpha_{\hat{m}}$ is the angle of rotation about an axis $\hat{m}=(\hat{z}\wedge\hat{n})/|\hat{z}\wedge\hat{n}|$ and $\vec{\underline{J}}$ is the total angular momentum. The torque quantity $T^{(\hat{n})}_{\alpha_{\hat{u}}}=-\frac{\partial F^{(\hat{n})}}{\partial\alpha_{\hat{u}}}$, describing the variation of the total energy with respect to a rotation of the magnetization about an axis $\hat{u}$, is

$$T^{(\hat{n})}_{\alpha_{\hat{u}}} = -\frac{1}{\pi}\int d\varepsilon f_{\mathrm{FD}}(\varepsilon;\nu^{(\hat{n})})\mathrm{Im}\,\frac{\partial}{\partial\alpha_{\hat{u}}}\{\ln\det[\underline{\underline{t}}(\hat{n};\varepsilon)^{-1}-\underline{\underline{G}}_0(\varepsilon)]\} \tag{A4}$$

which can be written

$$T^{(\hat{n})}_{\alpha_{\hat{u}}} = -\frac{1}{\pi}\int d\varepsilon f_{\mathrm{FD}}(\varepsilon;\nu^{(\hat{n})})\mathrm{Im}\sum_i \mathrm{tr}\Bigg(\underline{\underline{\tau}}^{(\hat{n})}_{ii}(\varepsilon) \times\frac{\partial}{\partial\alpha_{\hat{u}}}[\underline{R}(\hat{n})\underline{t}(\hat{z};\varepsilon)^{-1}\underline{R}(\hat{n})^+]\Bigg). \tag{A5}$$

Since $\frac{\partial\underline{R}(\hat{n})}{\partial\alpha_{\hat{u}}}=i(\vec{\underline{J}}\cdot\hat{u})\underline{R}(\hat{n})$ and $\frac{\partial\underline{R}(\hat{n})^+}{\partial\alpha_{\hat{u}}}=-i(\vec{\underline{J}}\cdot\hat{u})\underline{R}(\hat{n})^+$,

$$T^{(\hat{n})}_{\alpha_{\hat{u}}} = \frac{1}{\pi}\int d\varepsilon f_{\mathrm{FD}}(\varepsilon;\nu^{(\hat{n})})\mathrm{Im}\,i\sum_i \mathrm{tr}\{\underline{\underline{\tau}}^{(\hat{n})}_{ii}(\varepsilon)[(\underline{J}\cdot\hat{u})\underline{t}(\hat{n};\varepsilon)^{-1} - \underline{t}(\hat{n};\varepsilon)^{-1}(\underline{J}\cdot\hat{u})]\}. \tag{A6}$$

For $T^{(\hat{n})}_{\vartheta(\varphi)}$, $(\vec{\underline{J}}\cdot\hat{u})$ is just $\underline{J}_{y(z)}$.

Consider now our finite temperature torque expression, Eq. (38), i.e.,

$$T_\alpha = \frac{\mathrm{Im}}{\pi}\int d\varepsilon f_{\mathrm{FD}}(\varepsilon;\nu^{(\hat{n})})\sum_i\int\frac{\partial P^{(\hat{n})}_i(\hat{e}_i)}{\partial\alpha}\ln\det\underline{M}^{(\hat{n})}_i(\varepsilon;\hat{e}_i)d\hat{e}_i, \tag{A7}$$

with $\alpha=\vartheta$ or $\varphi$ and

$$\underline{M}^{(\hat{n})}_i(\varepsilon;\hat{e}_i) = \underline{I} + [\underline{t}_i(\varepsilon;\hat{e}_i)^{-1} - \underline{t}^{(\hat{n})}_{i,c}(\varepsilon)^{-1}]\underline{\underline{\tau}}^{(\hat{n})}_{ii,c}(\varepsilon). \tag{A8}$$

By definition,

$$T_\alpha = \frac{\mathrm{Im}}{\pi}\int d\varepsilon f_{\mathrm{FD}}(\varepsilon;\nu^{(\hat{n})})\sum_i\int\lim_{\Delta\alpha\to0}\frac{P^{(\hat{n}+\Delta\hat{n})}_i(\hat{e}_i)-P^{(\hat{n})}_i(\hat{e}_i)}{\Delta\alpha} \times\ln\det\underline{M}^{(\hat{n})}_i(\varepsilon;\hat{e}_i)d\hat{e}_i \tag{A9}$$

$$= \frac{\mathrm{Im}}{\pi}\int d\varepsilon f_{\mathrm{FD}}(\varepsilon;\nu^{(\hat{n})})\sum_i\lim_{\Delta\alpha\to0}\frac{1}{\Delta\alpha}\Bigg(\int P^{(\hat{n}+\Delta\hat{n})}_i \times(\hat{e}_i)\ln\det\underline{M}^{(\hat{n})}_i(\varepsilon;\hat{e}_i)d\hat{e}_i - \int P^{(\hat{n})}_i(\hat{e}_i)\ln\det\underline{M}^{(\hat{n})}_i \times(\varepsilon;\hat{e}_i)d\hat{e}_i\Bigg). \tag{A10}$$

Approaching $T=0$,

$$P^{(\hat{n})}_i(\hat{e}_i)\to\delta(\hat{n}-\hat{e}_i),\quad \underline{t}_i(\varepsilon;\hat{e}_i)\to\underline{t}_i(\varepsilon;\hat{n}), \tag{A11}$$

$$P^{(\hat{n}+\Delta\hat{n})}_i(\hat{e}_i)\to\delta(\hat{n}+\Delta\hat{n}-\hat{e}_i),\quad \underline{t}_i(\varepsilon;\hat{e}_i)\to\underline{t}_i(\varepsilon;\hat{n}+\Delta\hat{n}), \tag{A12}$$

while

$$\ln\det\underline{M}^{(\hat{n})}_i(\varepsilon;\hat{e}_i)\to\mathrm{Tr}\{[\underline{t}_i(\varepsilon;\hat{e}_i)^{-1}-\underline{t}^{(\hat{n})}_i(\varepsilon)^{-1}]\underline{\underline{\tau}}^{(\hat{n})}_{ii}(\varepsilon)\}. \tag{A13}$$

Therefore,

$$T_\alpha = \frac{\mathrm{Im}}{\pi}\int d\varepsilon f_{\mathrm{FD}}(\varepsilon;\nu^{(\hat{n})})\sum_i\lim_{\Delta\alpha\to0}\frac{1}{\Delta\alpha} \tag{A14}$$

$$\times\mathrm{Tr}\{[\underline{t}_i(\varepsilon;\hat{n}+\Delta\hat{n})^{-1}-\underline{t}^{(\hat{n})}_i(\varepsilon)^{-1}]\underline{\underline{\tau}}^{(\hat{n})}_{ii,c}(\varepsilon)\} - \mathrm{Tr}\{[\underline{t}_i(\varepsilon;\hat{n})^{-1}-\underline{t}^{(\hat{n})}_i(\varepsilon)^{-1}]\underline{\underline{\tau}}^{(\hat{n})}_{ii}(\varepsilon)\} \tag{A15}$$

$$= \frac{\mathrm{Im}}{\pi}\int d\varepsilon f_{\mathrm{FD}}(\varepsilon;\nu^{(\hat{n})})\sum_i\lim_{\Delta\alpha\to0}\frac{1}{\Delta\alpha}\mathrm{Tr}\{[\underline{t}_i(\varepsilon;\hat{n}+\Delta\hat{n})^{-1} - \underline{t}_i(\varepsilon;\hat{n})^{-1}]\underline{\underline{\tau}}^{(\hat{n})}_{ii}(\varepsilon)\} \tag{A16}$$

$$= \frac{\mathrm{Im}}{\pi}\int d\varepsilon f_{\mathrm{FD}}(\varepsilon;\nu^{(\hat{n})})\sum_i\mathrm{Tr}\Bigg(\frac{\partial\underline{t}_i(\varepsilon;\hat{n})^{-1}}{\partial\alpha}\underline{\underline{\tau}}^{(\hat{n})}_{ii}(\varepsilon)\Bigg), \tag{A17}$$

which is equivalent to Eq. (A5).


[1] H. J. F. Jansen, Phys. Rev. B **59**, 4699 (1999).
[2] J. Kubler, *Theory of Itinerant Electron Magnetism* (Clarendon, Oxford, 2000).
[3] J. B. Staunton, Rep. Prog. Phys. **57**, 1289 (1994).
[4] S. S. A. Razee, J. B. Staunton, B. Ginatempo, F. J. Pinski, and E. Bruno, Phys. Rev. Lett. **82**, 5369 (1999).
[5] A. B. Shick, D. L. Novikov, and A. J. Freeman, Phys. Rev. B **56**, R14259 (1997).
[6] T. Burkert, O. Eriksson, P. James, S. I. Simak, B. Johansson, and L. Nordstrom, Phys. Rev. B **69**, 104426 (2004).
[7] B. Lazarovits, B. Ujfalussy, L. Szunyogh, G. M. Stocks, and P. Weinberger, J. Phys.: Condens. Matter **16**, S5833 (2004).
[8] X. Qian and W. Hubner, Phys. Rev. B **64**, 092402 (2001).
[9] I. Cabria, A. Ya. Perlov, and H. Ebert, Phys. Rev. B **63**, 104424 (2001).
[10] H. Kronmuller, R. Fischer, R. Hertel, and T. Leineweber, J. Magn. Magn. Mater. **175**, 177 (1997); M. E. Schabes, *ibid.* **95**, 249 (1991).

[11] D. V. Baxter, D. Ruzmetov, J. Scherschligt, Y. Sasaki, X. Liu, J. K. Furdyna, and C. H. Mielke, Phys. Rev. B **65**, 212407 (2002); K. Hamaya, T. Taniyama, Y. Kitamoto, R. Moriya, and H. Munekata, J. Appl. Phys. **94**, 7657 (2003); A. B. Shick, F. Maca, J. Masek, and T. Jungwirth, Phys. Rev. B **73**, 024418 (2006).

[12] H. B. Callen and E. Callen, J. Phys. Chem. Solids **27**, 1271 (1966); N. Akulov, Z. Phys. **100**, 197 (1936); C. Zener, Phys. Rev. **96**, 1335 (1954).

[13] J. B. Staunton, S. Ostanin, S. S. A. Razee, B. L. Gyorffy, L. Szunyogh, B. Ginatempo, and Ezio Bruno, Phys. Rev. Lett. **93**, 257204 (2004).

[14] O. Mryasov, U. Nowak, K. Y. Guslienko, and R. W. Chantrell, Europhys. Lett. **69**, 805 (2005); R. Skomski, O. N. Mryasov, J. Zhou, and D. J. Sellmyer, J. Appl. Phys. **99**, 08E916 (2006).

[15] X. W. Wu, K. Y. Guslienko, R. W. Chantrell, and D. Weller, Appl. Phys. Lett. **82**, 3475 (2003).

[16] J.-U. Thiele, K. R. Coffey, M. F. Toney, J. A. Hedstrom, and A. J. Kellock, J. Appl. Phys. **91**, 6595 (2002).

[17] S. Okamoto, N. Kikuchi, O. Kitakami, T. Miyazaki, Y. Shimada, and K. Fukamichi, Phys. Rev. B **66**, 024413 (2002).

[18] *Electron Correlations and Magnetism in Narrow Band System*, edited by T. Moriya (Springer, New York, 1981).

[19] B. L. Gyorffy, A. J. Pindor, J. Staunton, G. M. Stocks, and H. Winter, J. Phys. F: Met. Phys. **15**, 1337 (1985).

[20] J. B. Staunton and B. L. Gyorffy, Phys. Rev. Lett. **69**, 371 (1992).

[21] S. Sun, C. B. Murray, D. Weller, L. Folks, and A. Moser, Science **287**, 1989 (2000).

[22] R. C. O'Handley, *Modern Magnetic Materials* (Wiley, New York, 2000).

[23] A. Lyberatos and K. Y. Guslienko, J. Appl. Phys. **94**, 1119 (2003); H. Saga, H. Nemoto, H. Sukeda, and M. Takahashi, Jpn. J. Appl. Phys., Part 1 **38**, 1839 (1999); M. Alex, A. Tselikov, T. McDaniel, N. Deeman, T. Valet, and D. Chen, IEEE Trans. Magn. **37**, 1244 (2001).

[24] O. A. Ivanov, L. V. Solina, V. A. Demshina, and L. M. Magat, Fiz. Met. Metalloved. **35**, 92 (1973).

[25] R. F. Farrow, D. Weller, R. F. Marks, M. F. Toney, A. Cebollada, and G. R. Harp, J. Appl. Phys. **79**, 5967 (1996).

[26] S. S. A. Razee, J. B. Staunton, and F. J. Pinski, Phys. Rev. B **56**, 8082 (1997).

[27] V. Heine, Solid State Phys. **35**, 105 (1980); A. Oswald, R. Zeller, P. J. Braspenning, and P. H. Dederichs, J. Phys. F: Met. Phys. **15**, 193 (1985).

[28] S. Ostanin, J. B. Staunton, S. S. A. Razee, C. Demangeat, B. Ginatempo, and Ezio Bruno, Phys. Rev. B **69**, 064425 (2004).

[29] S. Ostanin, S. S. A. Razee, J. B. Staunton, B. Ginatempo, and Ezio Bruno, J. Appl. Phys. **93**, 453 (2003); J. B. Staunton, S. Ostanin, S. S. A. Razee, B. Gyorffy, L. Szunyogh, B. Ginatempo, and Ezio Bruno, J. Phys.: Condens. Matter **16**, S5623 (2004).

[30] X. Wang, R. Wu, D. S. Wang, and A. J. Freeman, Phys. Rev. B **54**, 61 (1996).

[31] A. I. Akhiezer, V. G. Baryakhtar, and S. V. Peletminskii, *Spin Waves and Magnetic Excitations* (North-Holland, Amsterdam, 1968).

[32] E. Bruno and B. Ginatempo, Phys. Rev. B **55**, 12946 (1997).

[33] J. Korringa, Physica (Amsterdam) **13**, 392 (1947); W. Kohn and N. Rostoker, Phys. Rev. **94**, 1111 (1954).

[34] G. M. Stocks, W. M. Temmerman, and B. L. Gyorffy, Phys. Rev. Lett. **41**, 339 (1978).

[35] G. M. Stocks and H. Winter, Z. Phys. B: Condens. Matter **46**, 95 (1982); D. D. Johnson, D. M. Nicholson, F. J. Pinski, B. L. Gyorffy, and G. M. Stocks, Phys. Rev. Lett. **56**, 2088 (1986).

[36] S. S. A. Razee, J. B. Staunton, L. Szunyogh, and B. L. Gyorffy, Phys. Rev. Lett. **88**, 147201 (2002).

[37] M. F. Ling, J. B. Staunton, and D. D. Johnson, Europhys. Lett. **25**, 631 (1994).

[38] J. B. Staunton, M. F. Ling, and D. D. Johnson, J. Phys.: Condens. Matter **9**, 1281 (1997).

[39] V. Crisan, P. Entel, H. Ebert, H. Akai, D. D. Johnson, and J. B. Staunton, Phys. Rev. B **66**, 014416 (2002).

[40] M. Luders, A. Ernst, M. Dane, Z. Szotek, A. Svane, D. Kodderitzsch, W. Hergert, B. L. Gyorffy, and W. M. Temmerman, Phys. Rev. B **71**, 205109 (2005).

[41] I. D. Hughes, M. Daene, A. Ernst, W. Hergert, M. Lueders, J. Poulter, J. B. Staunton, A. Svane, Z. Szotek, and W. M. Temmerman (unpublished).

[42] K. Sato, P. H. Dederichs, H. Katayama-Yoshida, and J. Kudrnovsky, J. Phys.: Condens. Matter **16**, S5491 (2004).

[43] A. M. N. Niklasson, J. M. Wills, M. I. Katsnelson, I. A. Abrikosov, O. Eriksson, and B. Johansson, Phys. Rev. B **67**, 235105 (2003).

[44] D. A. Rowlands, J. B. Staunton, and B. L. Gyorffy, Phys. Rev. B **67**, 115109 (2003).

[45] D. A. Rowlands, A. Ernst, B. L. Gyorffy, and J. B. Staunton, Phys. Rev. B **73**, 165122 (2006).

[46] R. P. Feynman, Phys. Rev. **97**, 660 (1955).

[47] P. Soven, Phys. Rev. **156**, 809 (1967).

[48] A. Messiah, *Quantum Mechanics* (North-Holland, Amsterdam, 1965).

[49] P. Strange, J. Staunton, and B. L. Gyorffy, J. Phys. C **17**, 3355 (1984).

[50] B. L. Gyorffy and M. J. Stott, in *Band Structure Spectroscopy of Metals and Alloys*, edited by D. J. Fabian and L. M. Watson (Academic, New York, 1973).

[51] B. Ginatempo and J. B. Staunton, J. Phys. F: Met. Phys. **18**, 1827 (1988).

[52] P. Lloyd and P. R. Best, J. Phys. C **8**, 3752 (1975).

[53] J. S. Faulkner and G. M. Stocks, Phys. Rev. B **21**, 3222 (1980).

[54] A. Buruzs, L. Szunyogh, L. Udvardi, P. Weinberger, and J. B. Staunton (unpublished).

[55] J. B. Staunton, J. Poulter, B. Ginatempo, E. Bruno, and D. D. Johnson, Phys. Rev. B **62**, 1075 (2000).

[56] L. Wang, Z. Fan, A. G. Roy, and D. E. Laughlin, J. Appl. Phys. **95**, 7483 (2004).

[57] A. Ye. Yermakov and V. V. Maykov, Fiz. Met. Metalloved. **69**, 198 (1990); H. Shima, K. Oikawa, A. Fujita, K. Fukamichi, K. Ishida, and A. Sakuma, Phys. Rev. B **70**, 224408 (2004).

[58] G. H. O. Daalderop, P. J. Kelly, and M. F. H. Schuurmans, Phys. Rev. B **44**, 12054 (1991); I. V. Solovyev, P. H. Dederichs, and I. Mertig, *ibid.* **52**, 13419 (1995); I. Galanakis, M. Alouani, and H. Dreysse, *ibid.* **62**, 6475 (2000); D. Garcia, R. Casero, M. Vazquez, and A. Hernando, *ibid.* **63**, 104421 (2001).

[59] T. Burkert, O. Eriksson, S. I. Simak, A. V. Ruban, B. Sanyal, L. Nordstrom, and J. M. Wills, Phys. Rev. B **71**, 134411 (2005).

[60] H. Shima, K. Oikawa, A. Fujita, K. Fukamichi, and K. Ishida, J. Magn. Magn. Mater. **272**, 2173 (2004).

[61] K. Inoue, H. Shima, A. Fujita, K. Ishida, K. Oikawa, and K. Fukamichi, Appl. Phys. Lett. **88**, 102503 (2006).

[62] H. Gengnagel and U. Hoffmann, Phys. Status Solidi **29**, 91

(1968).
[63] O. Fruchert, J-P. Nozieres, and D. Givord, J. Magn. Magn. Mater. **165**, 508 (1997).
[64] C. Antoniak, J. Lindner, and M. Farle, Europhys. Lett. **70**, 250 (2005).
[65] J. Zabloudil, R. Hammerling, L. Szunyogh, and P. Weinberger, in *Electron Scattering in Solid Matter*, Springer Series in Solid State Sciences, Vol. 147 (Springer, Heidelberg, 2005).
[66] H. Ebert, S. Bornemann, J. Minar, P. H. Dederichs, R. Zeller, and I. Cabria, Comput. Mater. Sci. **35**, 279 (2006).